Sudden Unison: Quantitative Analysis of Chimera State Collapse and Epileptic Seizures

Henry Mitchell[1,2], Chris Danforth[1,4], and Matt Mahoney[3,4]

[1]Department of Mathematics and Statistics, University of Vermont College of Engineering and Mathematical Sciences
[2]Department of Physics, University of Vermont College of Arts and Sciences
[3]Department of Neurology, University of Vermont Larner College of Medicince
[4]Department of Computer Science, University of Vermont College of Engineering and Mathematical Sciences

March 25, 2019

Abstract

Contents

Chapter 1

Introduction

Pick better title

1.1 Chimera States

Italicize terms.

The science and mathematics of synchronization are among history's most well-studied areas of research. One of the earliest well-documented appearances of synchrony in unexpected places was observed in 1665 by Dutch physicist Christiaan Huygens, the inventor of the pendulum clock. He noticed that two clocks hung from the same beam would eventually synchronize with each other. He supposed that this was due to minuscule energy transfers between the two clocks through the wooden beam. This hypothesis was proven nearly 350 years later which shows that even the simplest-seeming synchronization behavior results from complex dynamics [17].

Put this in bibtex

This behavior extends to larger systems that two clocks. A classic demonstration in many classes on the mathematics of synchronization depicts the same phenomenon with more oscillators [16]. One places a platform on top of a set of rollers, and places at least two metronomes on that platform (see fig. 1.1 for a drawing). When these metronomes are started with the same frequency, out of phase with each other, over time their phases drift until they synchronize.

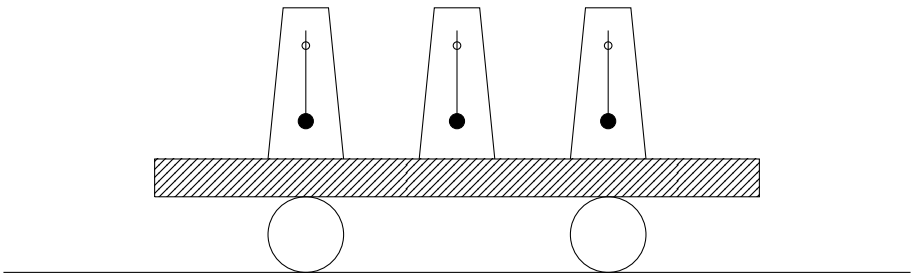

Figure 1.1: The classic demonstration of Huygens synchronization. When the metronomes are set running, they eventualy synchronize due to the light coupling provided by the platform's ability to roll.

One example of more complex behavior arising from similar mechanisms is the coexistence of synchrony and asynchrony within a system of identical coupled oscillators, a phenomenon

known as a chimera state [1, 12]. The existence of these chimera states are surprising, as they represent asymmetry within symmetric systems. The first time this behavior was observed was in a ring of nonlocally coupled oscillators [12]. The model is expressible in one dimension as

$$\frac{\partial}{\partial t}A(x,t) = (1+i\omega_0)A - (1+ib)|A|^2A + K(1+ia)(Z(x,t) - A(x,t)) \tag{1.1}$$

where

$$Z(x,t) = \int G(x-x')A(x',t)\,\mathrm{d}x' \quad \text{and} \quad G(y) = \frac{\kappa}{2}e^{-k|y|}, \tag{1.2}$$

which reduces to the phase equation

$$\frac{\partial}{\partial t}\phi(x,t) = \omega - \int G(x-x')\sin(\phi(x,t) - \phi(x',t) + \alpha)\,\mathrm{d}x' \quad \text{where} \quad \tan(\alpha) = \frac{b-a}{1+ab}. \tag{1.3}$$

When numerically simulated, this system quickly falls into a chimera state (fig. 1.2).

Fill in time and position.

(a) The time series of the Kuramoto simulation. (b) A snapshot at $t =$.

Figure 1.2: The results of a simulation of a Kuramoto oscillator, as described in eq. (1.3). A 4th-order Runge-Kutta solver ($\mathrm{d}t = 0.01$, $t_{\max} = 1000$) was run on a system of 512 oscillators. Figure 1.2a shows the entire time series of the simulation. The behavior represented there is quite complex, with several distinct qualitative changes to the patterns in the system. However, in-depth analysis of this system is beyond the purview of this work. Figure 1.2b shows a snapshot of the state of the system at $t =$. Note the juxtaposition of asynchronous (oscillators RANGE) and synchronous (oscillators RANGE).

Since then, chimera states have been found in simpler systems still. One of the simplest is the Abrams model, two populations of identical oscillators with a stronger coupling strength within the populations than between them [2]. The equation describing this system is given as

$$\frac{\mathrm{d}\theta_i^\sigma}{\mathrm{d}t} = \omega + \sum_{\sigma'=1}^{2}\frac{K_{\sigma\sigma'}}{N_{\sigma'}}\sum_{j=1}^{N_{\sigma'}}\sin\left(\theta_j^{\sigma'} - \theta_i^\sigma - \alpha\right) \quad \text{where} \quad K = \begin{bmatrix}\mu & \nu\\ \nu & \mu\end{bmatrix} \quad \text{and} \quad \sigma \in \{1,2\}. \tag{1.4}$$

In this model, μ represents the intra-population strength, and ν represents the inter-population strength, meaning $\mu > \nu$. Time can be scaled such that $\mu + \nu = 1$. If $\mu - \nu$ is not too large, and α is not too much less than $\frac{\pi}{2}$, then this system can produce chimera states.

Insert pictures

A similar system was also analyzed in the physical world [14]. Two swinging platforms were coupled together with springs of variable spring constant κ, and 15 metronomes—all tuned to the same frequency—were placed on each platform. For a wide range of values of κ, all of the metronomes on one platform would synchronize, while the metronomes on other platform would remain asynchronous. This system is directly analogous to the Abrams model. The metronomes on the same platform are coupled through the motion of the swing, which heavily influences the motion of the metronomes. This intra-community coupling is represented by μ in the Abrams model. The metronomes on opposite platforms are coupled

through the springs, which is a much weaker interaction, represented in the Abrams model by ν.

Chimera states have been observed in many other systems, whether they be purely mathematical, biological, electrical, or mechanical [1, 3, 8, 11, 12, 14, 15, 18–20, 24].

Find a transition.

1.2 Seizures

1.2.1 Neuroanatomy and Neurophysiology

Since the brain is an electrochemical device, its function and disorders are often best talked about from an electrical standpoint. *Neurons* are cells which are specialized for communication (see fig. 1.3 for a diagram). They receive input signals through *synapses* at the ends

Cite

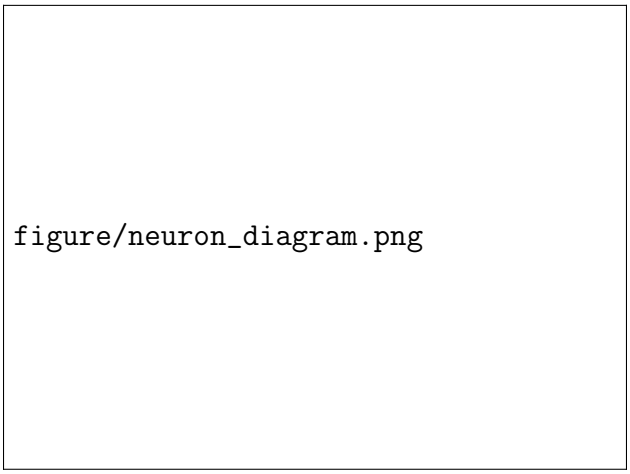

Figure 1.3: A diagram of the anatomy of a neuron.

of their *dendrites*, branches in their large tree of inputs. The trunk of the dendritic tree is the *soma*, the cell body. If the sum signal entering the soma from all of the dendrites is sufficient, the neuron *fires*, sending a signal to its outputs.

When a neuron fires, it sends an electrochemical signal down its *axon*—its long stem—to the output synapses at its *axon terminals*. This signal is known as an *action potential*. The action potential is discrete; a neuron sends the same signal any time its input threshold is surpassed, no matter how far above the threshold the input is. It is the propagation along the axon of a potential difference across the cell membrane of the neuron. This potential difference is created by different concentrations of various ions in and out of the cell, controlled by pumps (which push Na^+ out of the cell and draw K^+ into it) and gates (which allow the ion concentrations to equilibrate). It is important to note that processes involving Na^+ are faster than those involving K^+. Each location along the axon goes through the following six stages, in total taking approximately 1 ms:

Equilibrium No current flows through the membrane, which has a potential of $-75\,\mathrm{mV}$ across it[1].

[1] All potentials hold the extracellular matrix at 0 V. In other words, the interior of the cell is at a lower potential than the exterior.

Depolarization The potential difference propagating from upstream in the axon activates ion channel gates, allowing Na^+ to flow into the axon, countered by the K^+ flowing out.

Amplification Because the K^+ processes are slower than the Na^+ processes, if the incoming signal is strong enough, the influx of Na^+ is too fast for the outflow of K^+ to compensate. This results in a positive feedback loop, wherein the Na^+ flowing in increases the membrane potential, which increases the rate at which Na^+ flows into the neuron, which continues to feed itself.

Repolarization When the Na^+ channels are fully open, the K^+ channels are finally able to compensate for the influx.

Hyper-polarization The Na^+ channels close, and the slower K^+ channels remain open. This causes more K^+ to flow out of the cell than Na^+ flowed in, dropping the potential below its equilibrium state.

Refractory Period The Na^+ channels are briefly unable to open, which means that neurons need a brief time to "recharge" after an action potential.

Micro-scale models

All of these processes are summarized in the *Hodgkin-Huxley model*[2] describing the membrane potential U:

$$C_m\dot{U} + p_{AK^+}\bar{g}_{AK^+}(U - E_{K^+}) + p_{ANa^+}\bar{g}_{ANa^+}(U - E_{Na^+}) + g_l(U - E_l) = I_m \tag{1.5}$$

where

$$\begin{aligned} \dot{n} &= \alpha_n(1-n)\beta_n n \\ \dot{m} &= \alpha_m(1-m)\beta_m m \\ \dot{h} &= \alpha_h(1-h)\beta_h h \end{aligned} \quad \text{and} \quad \begin{aligned} p_{AK^+} &= n^4 \\ p_{ANa^+} &= m^3 h \end{aligned} \tag{1.6}$$

where g_i is the conductance of the membrane to ion i, p_{Ai} is the proportion of i-gates which are open (developed from a Markov model with transition rates α and β), E_i is the equilibrium potential of ion i, C_m is the capacitance of the membrane, and I_m is an external current (the tuned input parameter). This model is highly accurate, and won its developers a Nobel Prize in Physiology or Medicine. Many bifurcation analyses have been performed on these equations, and they are well understood [7].

However, the Hodgkin-Huxley model is not particularly useful for large-scale brain simulation. Given that most behavior of the brain is emergent[3], it is important to understand neurons' interactions. As is often the case with emergent phenomena, it is wildly impractical to simulate the collective behavior of a brain by simulating its constituent neurons. Since the human brain has approximately 10^{11} neurons with 10^{14} synapses, direct simulation is too computationally intensive. In order to better understand the dynamics of large portions of the brain, many researchers turned to the techniques of thermal and statistical physics

[2] A full derivation of this model can be found in [7].

[3] One of the classic ways to explain emergence is asking, "Where is the thought in a neuron?"

[5]. Particularly, *neural ensemble models* and *neural mass models* are popular approaches to studying brain behavior.

Meso-scale Models

Neural ensemble models treat patches of the brain as a collective group, taking into account neurons' mean activity, as well as their variance. They assume that the firings of the neurons within a group are sufficiently uncorrelated to result in a Gaussian distribution of firing rates. This means that the behavior of the ensemble is linear, even though the behavior of the constituent neurons is highly nonlinear. One can then use a Fokker-Planck equation to describe the collective dynamics of the population. The main benefit to these models is that they are well-studied in fields like solid-state physics. However, recent work has shown that the assumption of Gaussian firing rates is not accurate [5]. Firing rates do tend to fall into well-behaved distributions, but not ones that lend themselves to already-developed tools.

For higher coherence within populations (i.e., a non-Gaussian distribution of firing rates), researchers tend to use neural mass models. They assume that nearby neurons in the brain are sufficiently synchronized to model groups of them as a single neuron, with some modifications. Instead of the discrete action potential of a single neuron, neural mass models often have a sigmoidal activation function. They will also simplify the dynamics of the Hodgkin-Huxley model to divide the neural mass's constituent neurons into two subpopulations: an excitatory pool (corresponding to the Na^+ channels in the Hodgkin-Huxley model) and an inhibitory pool (corresponding to the K^+ channels in the Hodgkin-Huxley model).

And example of a neural mass model is the extremely simple Wilson-Cowan model [22]:

$$\tau_x \dot{x} = -xS(C_{xx}x + C_{xy}y + C_{xz}z + P) \tag{1.7}$$
$$\tau_y \dot{y} = -yS(C_{yx}x + C_{yy}y + C_{yz}z + Q) \tag{1.8}$$
$$\tau_z \dot{z} = -zS(C_{zx}x + C_{zy}y + C_{zz}z + R) \tag{1.9}$$

x represents an excitatory process (like the flow of Na^+), and y and z represent inhibitory processes (like the flow of K^+). The time constants τ_i determine the rates of the dynamics of the three processes. It is worth noting that chaotic dynamics can occur when multiple different time scales are present [5]. The coupling strengths C_{ij} represent the connectivity between the three processes, with $C_{ix} \geq 0$ (making x excitatory) and $C_{i\{y,z\}} \leq 0$ (making y inhibitory). P, Q, and R represent the excitability threshold, or the constant external inputs to each process (similar to I_m in eq. (1.5)). The sigmoidal activation function $S(x) = \frac{1}{1+e^{-a(x-\theta)}}$ represents the mass effect of the population of neurons being modeled. This system provides an excellent toy model which reflects meso-scale dynamics accurately, relative to its simplicity.

Macro-scale Models

These models do an accurate job of representing the behavior of small parts of the brain. However, it is not reasonable to carry the assumptions of un- or highly-correlated activity to the large-scale activity of whole-brain dynamics. In order to make these models accurately depict the overall behavior of the brain as a whole, researchers turn to two main techniques:

neural field models and *neural mass networks*. The first treats the brain as a continuous sheet of cortex, within which activity obeys wave equations. The second represents the brain as a discrete graph of cortices, or a network of coupled oscillators. An example of a neural mass network model is the modified Hindmarsh-Rose model (eqs. (3.1) to (3.3)), which is discussed later.

One of the benefits of a neural mass network model is that its outputs are similar to those of an *electroencephalograph*, or *EEG*. The EEG is a device used to record the electrical activity of the brain. Electrodes are placed in specific areas on the scalp, and then measure changes in voltage from neural masses beneath the skull. Much of the signal is distorted and attenuated by the bone and tissue between the brain and the electrodes, which act like resistors and capacitors. This means that, while the membrane voltage of the neuron changes by millivolts, the EEG reads a signal in the microvolt scale [23]. Additionally, the EEG has relatively low spatial and temporal resolution (16 electrodes for the whole brain, and a sampling rate of 33 ms). However, when properly treated, neural mass models make for effective predictors of the output from EEGs [13, 21]. This is useful, as EEGs are the main tool used to detect and categorize seizures.

1.2.2 Seizure Ætiology

For centuries, and across many cultures, seizures were viewed as holy and mystical events, and those with epilepsy were often considered to be shamans [6, 23]. Seizures are often accompanied by strange visions, sounds, or smells (called *auras*), and sometimes manifest themselves physically in extreme ways. External symptoms can include convulsions of the limbs or the entire body, or a seeming trance. In societies that are unfamiliar with the root causes of seizures, this can be a terrifying and awe-inspiring sight to behold.

In more recent years, researchers have come to define seizures as abnormal, excessive, or overly-synchronized neural activity [4, 23]. It is important to distinguish between seizures and epilepsy, as the two are often conflated. Seizures are an acute event, whereas epilepsy is a chronic condition of repeated seizures. While classification schemes vary, all center around the division between *generalized* and *focal* seizures.

Generalized seizures involve the entire brain, and start in both hemispheres at the same time, which is why they are often called *primary generalized seizures*. The manifestation of these seizures crosses an entire spectrum. They sometimes hardly present to an external observer, as in the case of the *typical absence seizure*[4], which is nonconvulsive and results in a complete cessation of motor activity for approximately 10 seconds. Patients lose consciousness, but not posture, making it seem to an observer like a trance or simply "spacing out."

On the other side of the range is the *tonic-clonic seizure*, wherein effectively all of a patient's muscles contract at once for around 30 seconds (the tonic phase), and then clench and unclench rapidly, resulting in jerking of the extremities (the clonic phase) for 1 to 2 minutes. After tonic-clonic seizures (in the *postictal* phase), patients often report confusion, muscle soreness, and exhaustion.

[4]Since a lot of early epilepsy research was performed in French-speaking regions, "absence" is pronounced æbˈsɑns.

Focal seizures start in one part of the brain (the seizure *focus*). They are generally preceded by auras such as a sense of fear, or hearing music, and often manifest as clonic movement of the extremities. In many cases, they secondarily generalize, spreading to the entire brain. This can make focal seizures and primary generalized seizures hard to distinguish, as a focal seizure can generalize rapidly after a brief aura. This can lead to misdiagnoses and improper treatments.

The Epileptor Model

From careful observation, an empirical/phenomenological seizure model called Epileptor was developed [9, 10]. It involves two fast processes x_1 and y_1, two *spike-wave event* processes x_2 and y_2, and a slow permittivity variable z. Its guiding equations are:

$$\dot{x}_1 = y_1 - f_1(x_1, x_2) - z + I_{\text{rest1}} \tag{1.10}$$

$$\dot{y}_1 = y_0 - 5x_1^2 - y_1 \tag{1.11}$$

$$\dot{z} = \frac{1}{\tau_0}(4(x_1 - x_0) - z) \tag{1.12}$$

$$\dot{x}_2 = -y_2 + x_2 - x_2^3 + I_{\text{rest2}} + 0.002g(x_1) - 0.3(z - 3.5) \tag{1.13}$$

$$\dot{y}_2 = \frac{1}{\tau_2}(-y_2 + f_2(x_1, x_2)) \tag{1.14}$$

where

$$g(x_1) = \int_{t_0}^{t} e^{-\gamma(t-\tau)} x_1(\tau)\,\mathrm{d}\tau \tag{1.15}$$

$$f_1(x_1, x_2) = \begin{cases} x_1^3 - 3x_1^2 & x_1 < 0 \\ x_1\big(x_2 - 0.6(z-4)^2\big) & x_1 \geq 0 \end{cases} \tag{1.16}$$

$$f_2(x_1, x_2) = \begin{cases} 0 & x_2 < -0.25 \\ 6(x_2 + 0.25) & x_2 \geq -0.25 \end{cases} \tag{1.17}$$

The required parameters have the following values: $x_0 = -1.6$, $y_0 = 1$, $\tau_0 = 2857$, $\tau_1 = 1$, $\tau_2 = 10$, $I_{\text{rest1}} = 3.1$, $I_{\text{rest2}} = 0.45$, $\gamma = 0.01$. An important matter to note is that $\tau_0 \gg \tau_2 \gg \tau_1$. As previously mentioned, these vastly different time scales allow for chaotic dynamics to occur, and contribute to the nonlinearity of the system.

While the Epileptor model is highly accurate, and is currently being used to develop patient-specific models and treatments, its main issue is that it is purely phenomenological. This means that it does not provide insight into the underpinnings and root causes behind seizures, simply describes symptoms.

Chapter 2

Literative Review

Chapter 3

Methods

3.1 Model

An example of a neural mass network is the modified Hindmarsh-Rose model [18].

$$\dot{x}_j = y_j - x^3 + bx_j^2 + I_j - z_j - \frac{\alpha}{n'_j}\sum_{k=1}^{N} G'_{jk}\Theta(x_k) - \frac{\beta}{n''_j}\sum_{k=1}^{N} G'_{jk}\Theta(x_k) \tag{3.1}$$

$$\dot{y}_j = 1 - 5x_j^2 - y_j \tag{3.2}$$

$$\dot{z}_j = \mu(s(x_j - x_{\text{rest}}) - z_j) \tag{3.3}$$

where

$$\Theta(x_k) = \frac{x_j - x_{\text{rev}}}{1 + e^{-\lambda(x_k - \theta)}} \tag{3.4}$$

In this model, x_j is the membrane potential of the jth neural mass, y_j is from the fast processes

Chapter 4

Results

List of Figures

Bibliography

[1] Daniel M. Abrams and Steven H. Strogatz. "Chimera States for Coupled Oscillators". In: *Physical Review Letters* 93.17 (Oct. 2004). DOI: 10.1103/physrevlett.93.174102. URL: https://doi.org/10.1103/physrevlett.93.174102.

[2] Daniel M. Abrams et al. "Solvable Model for Chimera States of Coupled Oscillators". In: *Physical Review Letters* 101.8 (Aug. 2008). DOI: 10.1103/physrevlett.101.084103. URL: https://doi.org/10.1103/physrevlett.101.084103.

[3] Ralph G. Andrzejak et al. "All together now: Analogies between chimera state collapses and epileptic seizures". In: *Scientific Reports* 6.1 (Mar. 2016). DOI: 10.1038/srep23000. URL: https://doi.org/10.1038/srep23000.

[4] Gerold Baier et al. "The importance of modeling epileptic seizure dynamics as spatiotemporal patterns". In: *Frontiers in Physiology* 3 (2012). DOI: 10.3389/fphys.2012.00281. URL: https://doi.org/10.3389/fphys.2012.00281.

[5] Michael Breakspear. "Dynamic models of large-scale brain activity". In: *Nature Neuroscience* 20.3 (Mar. 2017), pp. 340–352. DOI: 10.1038/nn.4497. URL: https://doi.org/10.1038/nn.4497.

[6] A. Fadiman. *The Spirit Catches You and You Fall Down: A Hmong Child, Her American Doctors, and the Collision of Two Cultures*. FSG Classics. Farrar, Straus and Giroux, 1998. ISBN: 9781429931113. URL: https://books.google.com/books?id=DUHAXXvSUeYC.

[7] P. Graben et al. *Lectures in Supercomputational Neuroscience: Dynamics in Complex Brain Networks*. Understanding Complex Systems. Springer Berlin Heidelberg, 2007. ISBN: 9783540731597. URL: https://books.google.com/books?id=GW36HNEs4ucC.

[8] Johanne Hizanidis et al. "Chimera-like States in Modular Neural Networks". In: *Scientific Reports* 6.1 (Jan. 2016). DOI: 10.1038/srep19845. URL: https://doi.org/10.1038/srep19845.

[9] V.K. Jirsa et al. "The Virtual Epileptic Patient: Individualized whole-brain models of epilepsy spread". In: *NeuroImage* 145 (Jan. 2017), pp. 377–388. DOI: 10.1016/j.neuroimage.2016.04.049. URL: https://doi.org/10.1016/j.neuroimage.2016.04.049.

[10] Viktor K. Jirsa et al. "On the nature of seizure dynamics". In: *Brain* 137.8 (June 2014), pp. 2210–2230. DOI: 10.1093/brain/awu133. URL: https://doi.org/10.1093/brain/awu133.

[11] Nikita Kruk, Yuri Maistrenko, and Heinz Koeppl. "Self-propelled chimeras". In: *Physical Review E* 98.3 (Sept. 2018). DOI: 10.1103/physreve.98.032219. URL: https://doi.org/10.1103/physreve.98.032219.

[12] Yoshiki Kuramoto and Dorjsuren Battogtokh. "Coexistence of Coherence and Incoherence in Nonlocally Coupled Phase Oscillators". In: *arXiv e-prints*, cond-mat/0210694 (Oct. 2002), cond–mat/0210694. arXiv: cond-mat/0210694 [cond-mat.stat-mech].

[13] Lutz Leistritz et al. "Coupled oscillators for modeling and analysis of EEG/MEG oscillations". In: *Biomedizinische Technik/Biomedical Engineering* 52.1 (Feb. 2007), pp. 83–89. DOI: 10.1515/bmt.2007.016. URL: https://doi.org/10.1515/bmt.2007.016.

[14] E. A. Martens et al. "Chimera states in mechanical oscillator networks". In: *Proceedings of the National Academy of Sciences* 110.26 (June 2013), pp. 10563–10567. DOI: 10.1073/pnas.1302880110. URL: https://doi.org/10.1073/pnas.1302880110.

[15] Mark J Panaggio and Daniel M Abrams. "Chimera states: coexistence of coherence and incoherence in networks of coupled oscillators". In: *Nonlinearity* 28.3 (Feb. 2015), R67–R87. DOI: 10.1088/0951-7715/28/3/r67. URL: https://doi.org/10.1088/0951-7715/28/3/r67.

[16] James Pantaleone. "Synchronization of metronomes". In: *American Journal of Physics* 70.10 (Oct. 2002), pp. 992–1000. DOI: 10.1119/1.1501118. URL: https://doi.org/10.1119/1.1501118.

[17] Jonatan Peña Ramirez et al. "The sympathy of two pendulum clocks: beyond Huygens' observations". In: *Scientific Reports* 6.1 (Mar. 2016). DOI: 10.1038/srep23580. URL: https://doi.org/10.1038/srep23580.

[18] M.S. Santos et al. "Chimera-like states in a neuronal network model of the cat brain". In: *Chaos, Solitons & Fractals* 101 (Aug. 2017), pp. 86–91. DOI: 10.1016/j.chaos.2017.05.028. URL: https://doi.org/10.1016/j.chaos.2017.05.028.

[19] M.S. Santos et al. "Recurrence quantification analysis of chimera states". In: *Physics Letters A* 379.37 (Oct. 2015), pp. 2188–2192. DOI: 10.1016/j.physleta.2015.07.029. URL: https://doi.org/10.1016/j.physleta.2015.07.029.

[20] Murray Shanahan. "Metastable chimera states in community-structured oscillator networks". In: *Chaos: An Interdisciplinary Journal of Nonlinear Science* 20.1 (Mar. 2010), p. 013108. DOI: 10.1063/1.3305451. URL: https://doi.org/10.1063/1.3305451.

[21] Peter Neal Taylor et al. "Towards a large-scale model of patient-specific epileptic spike-wave discharges". In: *Biological Cybernetics* 107.1 (Nov. 2012), pp. 83–94. DOI: 10.1007/s00422-012-0534-2. URL: https://doi.org/10.1007/s00422-012-0534-2.

[22] Yujiang Wang et al. "Phase space approach for modeling of epileptic dynamics". In: *Physical Review E* 85.6 (June 2012). DOI: 10.1103/physreve.85.061918. URL: https://doi.org/10.1103/physreve.85.061918.

[23] Gary L. Westbrook. "Principles of Neural Science". In: ed. by Eric R. Kandel et al. Fifth. McGraw Hill Medical, 2013. Chap. 50, pp. 1116–1139.

[24] Jianbo Xie, Edgar Knobloch, and Hsien-Ching Kao. "Multicluster and traveling chimera states in nonlocal phase-coupled oscillators". In: *Physical Review E* 90.2 (Aug. 2014). DOI: 10.1103/physreve.90.022919. URL: https://doi.org/10.1103/physreve.90.022919.